Investigation of the Mechanism of Phosphinothricin Inactivation of *Escherichia coli* Glutamine Synthetase Using Rapid Quench Kinetic Techniques†

Lynn M. Abell and Joseph J. Villafranca*

Department of Chemistry, The Pennsylvania State University, University Park, Pennsylvania 16802

Received November 19, 1990; Revised Manuscript Received March 7, 1991

ABSTRACT: A number of slow tight-binding inhibitors are known for glutamine synthetase that resemble the geometry of the tetrahedral intermediate formed during the enzyme-catalyzed condensation of γ-glutamyl phosphate and ammonia. One of these inhibitors, phosphinothricin [L-2-amino-4-(hydroxymethylphosphinyl)butanoic acid], has been investigated by rapid kinetic methods. Phosphinothricin not only exhibits the kinetic properties of a slow tight-binding inhibitor but also undergoes phosphorylation during the course of the ATP-dependent inactivation. The acid lability of phosphinothricin phosphate enabled investigation of the kinetics of glutamine synthetase inactivation using rapid quench kinetic techniques. The rate-limiting step in the inhibition reaction is the binding of inhibitor (0.004–0.014 μM^{-1} s^{-1}) and/or a conformational change associated with binding, which is several orders of magnitude slower than the binding of ATP. The association rate of phosphinothricin depends on which metal ion is bound to the enzyme (Mn^{2+} or Mg^{2+}). With Mn^{2+} bound to glutamine synthetase the rate of association and the phosphorylation rate are faster than when Mg^{2+} is bound. The data are interpreted with use of a model in which the binding of a substrate analogue with a tetrahedral moiety enhances the phosphorylation rate of the reaction intermediate; however, the initial binding interaction is retarded because the enzyme has to bind a molecule that has a "transition-state" geometry rather than a ground-state substrate structure. During the course of the inactivation, progressively slower rates for binding and phosphoryl transfer were observed, indicating communication between active sites.

Glutamine synthetase (GS)[1] from *Escherichia coli* catalyzes the ATP-dependent formation of glutamine from glutamate and ammonia (Stradman & Ginsburg, 1974).

$$\text{glutamate} + \text{ATP} + \text{NH}_3 \xrightleftharpoons{2M^{2+}} \text{glutamine} + \text{ADP} + \text{P}_i \quad (1a)$$

The enzyme has a molecular weight of 600 000 and is a dodecamer of identical subunits, which are arranged in two hexameric rings that are stacked on top of each other. GS requires two divalent metal ions for catalysis, which are clearly seen in the X-ray crystal structure and identify the 12 active sites. Each active site lies at the interface of two adjacent subunits in a given hexameric ring and is composed of the C-terminal domain of one subunit and the N-terminal domain of the other (Almassy et al., 1986; Yamashita et al., 1989). GS plays a central role in nitrogen metabolism in both prokaryotes and eukaryotes and is highly regulated by numerous feedback inhibitors and at the level of transcription by ammonia repression (Stadtman & Ginsburg, 1974). The enzyme from Gram negative bacteria such as *E. coli* is further regulated by a covalent adenylylation modification. Tyrosine 397 is modified by the enzyme adenylyl transferase in response to the level of glutamine and α-ketoglutarate in the cell (Ginsburg & Stadtman, 1973; Stadtman et al., 1980; Magasanik & Reitzer, 1987). The effect of the adenylylation modification is to elevate the K_m's for all substrates (Abell & Villafranca, 1991) and to change the metal ion specificity and pH required for optimal activity (Ginsburg et al., 1970). The unadenylylated enzyme shows optimal activity with Mg^{2+} at pH 7.5, and this is most likely the physiologically important metal ion. The adenylylated enzyme, however, shows maximal activity with Mn^{2+} at pH 6.5.

The chemical mechanism of glutamine synthetase involves the initial formation of a γ-glutamyl phosphate intermediate; this is followed by displacement of the activated phosphate group by ammonia through the formation of a phosphorylated tetrahedral intermediate (Scheme I).

The presence of the acid-labile γ-glutamyl phosphate intermediate was previously detected from the observation of a burst of acid-labile phosphate in a rapid quench experiment with low adenylylation state enzyme and Mg^{2+} as the activating metal (Meek et al., 1982). Use of this technique not only provided evidence for the intermediacy of γ-glutamyl phosphate but also offered some insight into the energetics of phosphoryl transfer.

A number of potent inhibitors are known for glutamine synthetase that mimic the geometry of the tetrahedral intermediate. Two of the most widely studied of these inhibitors are methionine sulfoximine (MSOX) and phosphinothricin (PPT) (Scheme II). Both inhibitors require the presence of ATP and metal ions for inactivation (Ronzio & Meister, 1968; Ronzio et al., 1969; Colanduoni & Villafranca, 1986). In the case of MSOX, it has been known for some time that the inhibitor undergoes a chemical modification during the course of the inactivation to form phosphorylated MSOX. The γ-phosphoryl group of ATP is transferred to the imine nitrogen group to form a final tight complex composed of MSOX-P

† This work was supported by NIH Grants GM23529 (J.J.V.) and GM11994 (fellowship to L.M.A.).

* To whom correspondence should be addressed.

[1] Abbreviations: GS, glutamine synthetase; GS(n = 2), low adenylylation state enzyme; GS(n = 12), high adenylylation state enzyme; MSOX, L-methionine-(*S*,*R*)-sulfoximine; MSOX-P, methionine-sulfoximine phosphate; PPT, L-2-amino-4-(hydroxymethylphosphinyl)butanoic acid; PPT-P, phosphinothricin phosphate; Hepes, *N*-(2-hydroxyethyl)-piperazine-*N*′-2-ethanesulfonic acid; PEP, phosphoenolpyruvate; EDTA, ethylenediaminetetraacetic acid; Pipes, piperazine-*N*,*N*′-bis(2-ethanesulfonic acid).

0006-2960/91/0430-6135$02.50/0

Scheme I

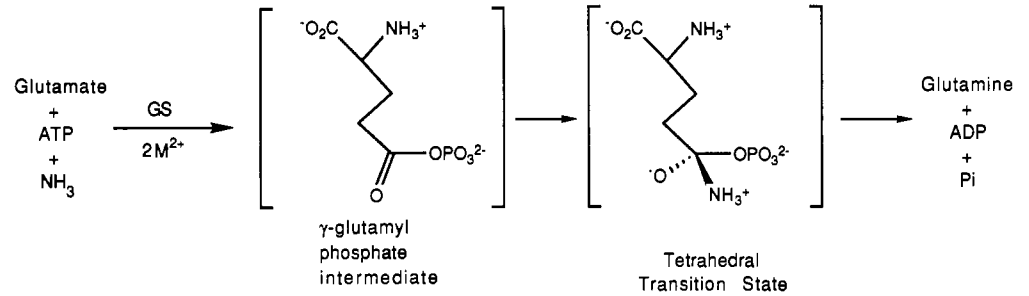

Scheme II

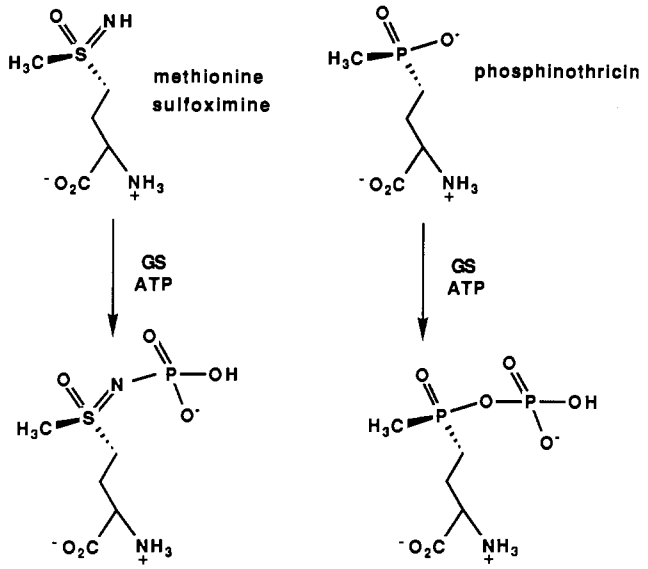

and ADP (Rowe et al., 1969). Under normal inactivation conditions, no reactivation is observed. However, the enzyme can be completely reactivated at pH 3.5–4.6 in 1 M KCl and 0.4 M ammonium sulfate (Maurizi & Ginsburg, 1982). The enzyme preferentially binds the L-(*S*)-MSOX diastereomer, and semilog plots of time-dependent inactivation data are curved, indicating that binding of the inhibitor exhibits negative cooperativity (Shrake et al., 1982). Negative cooperativity has also been observed in the normal biosynthetic reaction. Double-reciprocal plots with ammonia as the variable substrate are concave downward, indicating negative cooperativity in NH_4^+ binding (Meek & Villafranca, 1980).

Inactivation of glutamine synthetase with PPT was thought to proceed by a mechanism similar to that of MSOX. Inhibition by PPT also exhibited negative cooperativity (Logusch et al., 1989) and required a hydrolyzable analogue of ATP (Colanduoni & Villafranca, 1986). However, attempts to isolate phosphorylated PPT (PPT-P) in a manner similar to that of MSOX-P proved unsuccessful. Recently, PPT-P has been isolated and characterized by NMR by quenching the inactivation solution with base instead of acid (Schineller & Villafranca, 1991). The results of these experiments indicate that unlike MSOX-P, PPT-P is stable in base but unstable in acid.

For most slow tight-binding inhibitors, the mechanism of inactivation is thought to involve initial rapid formation of the enzyme–inhibitor complex followed by some slow step, possibly a conformational change, that makes the overall binding appear kinetically slow (Morrison & Walsh, 1988).

$$E + I \overset{\text{fast}}{\rightleftharpoons} EI \overset{\text{slow}}{\rightleftharpoons} E'I \qquad (1b)$$

MSOX and PPT differ from more traditional slow tight-binding inhibitors in that they not only bind very tightly to the enzyme and show time-dependent inactivation but also undergo chemical modification as well. In the case of glutamine synthetase inhibition, it is not known whether the slow step involves a conformational change, chemistry, or both. The acid lability of PPT-P makes it the perfect probe to investigate the kinetics of GS inactivation by rapid quench kinetic techniques. This technique can be used to determine if phosphoryl transfer plays a kinetically significant role in the inactivation process.

Recently, rapid quench experiments conducted on (1) low adenylylation state GS with either Mn^{2+} or Mg^{2+} and (2) adenylylated GS with Mn^{2+} have shown that in the biosynthetic reaction the affect of adenylylation is to change the rate-limiting step from product release to phosphoryl transfer (Abell & Villafranca, 1991). All three forms of the enzyme were used in the present experiments to determine the effect of adenylylation and metal ion on the inactivation kinetics with PPT. The kinetic analysis used for these experiments will be described in detail for GS(n = 2)Mn^{2+} at pH 6.5. Similar analyses were conducted with data from experiments with GS(n = 2)Mg^{2+} at pH 7.5 and GS(n = 12)Mn^{2+} at pH 6.5. The results for all three enzyme forms are compared and discussed.

Experimental Procedures

Materials. [γ-^{32}P]ATP (10–50 Ci/mmol) was obtained from New England Nuclear and purified prior to use according to Lewis and Villafranca (1989). Phosphinothricin (D,L) was a gift from Hoechst. Concentrations given for PPT refer to the L isomer throughout. All other biochemicals were from Sigma and were of the highest purity available.

Enzyme. Glutamine synthetase was purified from *E. coli* YMC10 (Backman et al., 1981) containing the plasmid pgln6. This plasmid contains *gln*A, the structural gene for glutamine synthetase. Low adenylylation state enzyme (GS(n = 2)) was obtained from the above mentioned YMC10/pgln6 cells grown on minimal media with glucose as the carbon source and glutamine as the sole nitrogen source. In the final growth, $MnCl_2$ was added to a final concentration of 1 mM to inhibit oxidation of GS (Roseman & Levine, 1987). The enzyme was purified with use of a variation of the zinc precipitation method (Miller et al., 1974), which included a streptomycin sulfate step, one zinc precipitation step followed by extensive dialysis to remove the zinc, an acetone precipitation step at 0 °C, and a final ammonium sulfate precipitation at pH 4.4 (Rhee et al., 1985).

Adenylylated enzyme (GS(n = 12)) was prepared in vitro by use of the enzyme adenylyl transferase (Hennig & Ginsburg, 1971) and then repurified by zinc precipitation and an ammonium sulfate precipitation.

Protein concentrations were determined by either the BCA assay (Pierce) in the absence of Mn^{2+} or by spectrophotometric methods (Ginsburg et al., 1970). Adenylylation state was

determined spectrophotometrically (Shapiro & Stadtman, 1970) and by the transferase assay method (Stadtman et al., 1979).

Low adenylylation state enzyme had an average adenylylation state of 1.4 ± 0.1 and a specific activity of 120 units/mg by the transferase assay. GS(n = 12) had an average adenylylation state of 12.1 ± 0.2 and a specific activity of 138 units/mg. Each enzyme was shown to be 95–98% pure by denaturing gel electrophoresis.

The Mn^{2+} form of the enzyme was converted to the Mg^{2+} form by dialysis against several changes of buffer containing EDTA for 12 h and then dialyzed extensively for 36 h against 50 mM Hepes or Pipes/100 mM KCl/25 mM $MgCl_2$ at the desired pH. The specific activity of the enzyme was found to be unchanged after this procedure.

Trapping Phosphinothricin Phosphate. Phosphorylated phosphinothricin was trapped by reacting 20 mg of enzyme with 2 mM PPT and 4 mM ATP in the presence of 100 mM KCl and either 8 mM Mn^{2+}/300 mM Pipes at pH 6.5 or 25 mM Mg^{2+}/200 mM Hepes at pH 7.5 in a total volume of about 800 μL. The reaction was allowed to proceed at room temperature for 30 min and was quenched by adding 500 μL of triethylamine and several drops of CCl_4. The sample was centrifuged for 15 min, and the middle aqueous layer was removed. EDTA (100 μL of a 0.45 mM solution) was added, and the sample was centrifuged again. The supernatant was removed, and 100 μL of D_2O was added. The ^{31}P NMR spectrum showed two sets of doublets, one centered at 52.40 ppm (J = 27.08 Hz, α-PPT-P) and the other at −4.28 ppm (J = 26.99 Hz, β-PPT-P) (Schineller & Villafranca, 1991).

Time-Dependent Enzyme Inactivation with PPT. The time course of inactivation of GS with PPT was measured at 25 °C by preincubating micromolar amounts of enzyme and inhibitor with ATP and metal at pH 6.5 (with Mn^{2+}) and pH 7.5 (with Mg^{2+}). Preincubation reactions carried out with GS(n = 2) with Mn^{2+} contained 8.3 μM unadenylylated subunits, a variable amount of inhibitor, 1.25 mM ATP, and 8 mM Mn^{2+} in 50 mM Pipes buffer with 100 mM KCl at pH 6.5. Similar conditions were used for GS(n = 12) with Mn^{2+} except that the enzyme concentration was only 5 μM. Each preincubation reaction carried out with GS(n = 2) with Mg^{2+} contained 1 μM unadenylylated subunits, a variable amount of inhibitor, 1.25 mM ATP, and 25 mM Mg^{2+} Hepes buffer with 100 mM KCl at pH 7.5. The amount of activity remaining after a given preincubation time was determined with use of a continuous assay in which ADP production was coupled to NADH oxidation with lactate dehydrogenase and pyruvate kinase. After specific preincubation times, an aliquot of the preincubation mixture was added to a cuvette containing 100 mM Hepes at pH 7.5 or 100 mM Pipes at pH 6.5, 100 mM KCl, 1 mM PEP, 190 μg of NADH, 33 μg/mL pyruvate kinase, 33 μg/mL L-lactate dehydrogenase, and saturating amounts of substrates (2 mM ATP, 50 mM glutamate, and 50 mM NH_3). For assays conducted at pH 6.5, 8 mM Mn^{2+} was used and for those at pH 7.5, 25 mM Mg^{2+} was present in the assay mix. One hundred percent activity was determined by use of several different methods. Enzyme was assayed after preincubation at 25 °C in the absence of inhibitor or in the absence of preincubation but in the presence of the same concentration of PPT in the cuvette that would result from dilution of a given preincubation mixture. Each method gave the same activity as assaying the enzyme alone and without any preincubation. Assays were performed in 1.0-cm cuvettes with 1.00-mL total volume in a Cary 2200 UV/vis spectrophotometer thermostatted at 25 °C. The change in absorbance at 340 nm vs time was monitored. Initial rates of reaction were determined with use of SPECTRA CALC.

Rapid Quench Experiments. The rapid quench experiments were performed at 25 °C on an apparatus designed and built by Johnson (1986). The reactions were initiated by the simultaneous mixing of two solutions, one containing enzyme and activating metal ion at the appropriate pH (0.039 mL), and the other containing all substrates (0.042 mL) and trace amounts of [γ-^{32}P]ATP (5000 cpm added per nmol of cold ATP). The reactions were quenched with 190 μL of 0.6 N HCl and then immediately neutralized with 45 μL of a solution containing 1 M Tris and 4 N KOH. [γ-^{32}P]P_i was isolated as described by Johnson (1986). Cold ATP concentrations were determined spectrophotometrically by measuring the absorbance at 259 nm of a 0.1 M solution prepared from the stock solution. Two sets of rapid quench experiments were conducted for each form of the enzyme, one containing micromolar amounts of enzyme and a 1–5 molar excess of PPT and a second experiment containing micromolar amounts of enzyme and 100 mM PPT. Data were collected from 100 ms to 15 s for the low PPT concentration experiments and from 5 ms to 1 s for the high PPT concentration experiments. For reactions in the presence of Mn^{2+}, the final reaction mixture contained 100 mM Pipes, 100 mM KCl, 8 mM Mn^{2+}, 1 mM PEP, 33 μg/mL pyruvate kinase, a variable amount of inhibitor as specified above, and 1 mM ATP at pH 6.5. For reactions in the presence of Mg^{2+}, the final reaction mixture contained the same components as above except that the buffer was 100 mM Hepes at pH 7.5 and 25 mM Mg^{2+} was substituted for Mn^{2+}.

Data Analysis. Time-dependent inactivation curves were fit to a double-exponential equation (eq 2) by use of the

$$\% \text{ activity remaining} = Ae^{-k_a t} + (100 - A)e^{-k_b t} \quad (2)$$

nonlinear regression analysis of Duggleby (1984). In eq 2, k_a is the rate constant for the initial phase of inactivation, k_b is the rate constant for the second phase of inactivation, and A is the population of active sites that are inactivated in either phase. Rapid quench data were fit by use of the computer program KINSIM (Barshop et al., 1983) to simulate the reaction pathway. The program was modified by Johnson to allow the input of data from rapid quench experiments as x,y pairs and to allow automated fitting and error analysis for individual rate constants by use of one or more sets of experimental data simultaneously.

Results

Trapping Phosphorylated Phosphinothricin. Phosphorylated phosphinothricin was trapped and observed by ^{31}P NMR for all three forms of the enzyme studied, GS(n = 2) with Mn^{2+} and Mg^{2+} and GS(n = 12) with Mn^{2+}. For the reactions involving Mn^{2+} as the activating metal ion, most of the Mn^{2+} was removed when the reactions were quenched with triethylamine and so the paramagnetic metal did not interfere with the NMR spectral determinations.

Time-Dependent Inactivation. Time-dependent inactivation studies were conducted by preincubating micromolar amounts of enzyme and PPT with metal and ATP and then diluting the preincubation mixture into assay solution that contained saturating amounts of substrates. The amount of activity remaining after a given preincubation time could then be measured. As has been observed by previous investigators, semilog plots of percent activity versus time were not linear (Logusch et al., 1989). In an attempt to fit the entire inactivation curve, time-dependent inactivation data were fit to eq 2. The results for GS(n = 2) with Mn^{2+} at pH 6.. and

Table I: Rate Constants from Double-Exponential Fits of PPT Inactivation of GS(n = 2) with Mn^{2+} at pH 6.5[a]

[PPT] (μM)	k_a (s^{-1})	k_b (s^{-1})	A
8.3	0.060 ± 0.003	0.0016 ± 0.0002	54.7 ± 1.3
9.3	0.060 ± 0.003	0.0021 ± 0.0004	54.4 ± 1.6
10.0	0.072 ± 0.008	0.0022 ± 0.0003	45.8 ± 2.1
12.0	0.074 ± 0.004	0.0025 ± 0.0002	53.0 ± 1.4
15.6	0.078 ± 0.008	0.0078 ± 0.002	64.5 ± 5.0

[a] Inactivation reactions were carried out at 25 °C with 8.3 μM of unadenylylated subunits.

Scheme III

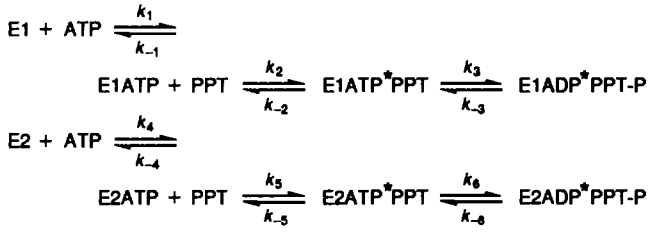

a small range of PPT concentrations are summarized in Table I. The range of PPT concentrations that could be used in these experiments was somewhat limited. At higher inhibitor concentrations, the inactivation became too fast to measure accurately. The results in Table I show that over the inhibitor concentration range investigated the fits to the double-exponential equation were good. The fast and slow phases of the inactivation seem to be roughly divided into equal populations. The inverse of the slope of double-reciprocal plots of k_a and k_b versus [PPT] give an estimate of the association rate for PPT for the two populations. For the initial phase of inactivation, k_{on} for PPT is 0.013 ± 0.001 μM^{-1} s^{-1} while in the final phase of inactivation k_{on} is 0.0002 ± 0.0001 μM^{-1} s^{-1}. A similar analysis of data from experiments with GS(n = 2) and Mg^{2+} at pH 7.5 and GS(n = 12) with Mn^{2+} at pH 6.5 gave populations around 60% for the initial phase and 40% for the slower phase.

Data analysis using eq 2 was somewhat limited by the fact that only data from a small range of PPT concentrations was available and this equation does not account for changes in free substrate and free enzyme concentrations during the course of the inactivation reaction. The analysis also only gives a rate constant for overall inactivation and cannot be used to distinguish the more subtle points of various possible mechanisms. For example, this analysis cannot distinguish between the two-step mechanism in eq 1b and a simple one-step mechanism where E + I leads to inactive enzyme directly. However, this analysis provided a useful starting model for more complete simulation of the data using KINSIM, which does not suffer from the above limitations.

The mechanism used for KINSIM simulations is shown in Scheme III. Two populations of enzyme are assumed: the first, E1, binds PPT with the rate constant k_2, and the second, E2, binds PPT with the slightly slower rate constant k_5. The association rate for ATP has previously been measured by stopped-flow fluorescence experiments (Abell & Villafranca, 1991; see Table II). k_3 and k_6 represent the phosphoryl transfer rates for the initial and final phases of inactivation.

Automated fitting and error analysis of the time-dependent inactivation data with respect to k_2 and k_5 and the assumption of a 50/50 population of enzyme gave k_2 = 0.014 ± 0.001 μM^{-1} s^{-1} and k_5 = 0.0004 ± 0.0001 μM^{-1} s^{-1}. These results are in good agreement with the estimates from the double-exponential analysis, indicating that the limitations of the above analysis were not significant. The simulation fit is superimposed on the experimental data in Figure 1. The population of enzyme undergoing the fast initial inactivation could be varied from 55 to 45% with the requisite variation in the second population without changing the association rates significantly and while still obtaining good fits to the data. Simulation of these data was insensitive to assumptions made about the phosphoryl-transfer rates, and the association rates did not change over a wide range of assumed rates for k_3 and k_6 (0.1–100 s^{-1}). This result is consistent with the fact that either EATP*PPT or EADP*PPT-P could be assumed as the inactive form of the enzyme in the KINSIM simulations with no change in the calculated association rates. Clearly, these data are insensitive to the rates of phosphoryl transfer, and rapid quench data must be used to determine these rates. The fits to the data were also insensitive to the values for k_{-2} and k_{-5} over a range of 0.0–0.9 s^{-1}. Accurate values could not be obtained for these rates.

Table II: Rate Constants from Fitting Rapid Quench Data for High and Low [PPT] for GS(n = 2) with Mn^{2+} at pH 6.5[a]

k_2 (μM^{-1} s^{-1})	k_3 (s^{-1})	k_5 (μM^{-1} s^{-1})	k_6 (s^{-1})
0.014 ± 0.001	245 ± 14	0.0004 ± 0.0001	36 ± 7

[a] For these experiments the kinetic constants previously measured by Abell and Villafranca (1991) were used ($k_1 = k_4$ = 4.22 μM^{-1} s^{-1} and $k_{-1} = k_4$ = 160 s^{-1}).

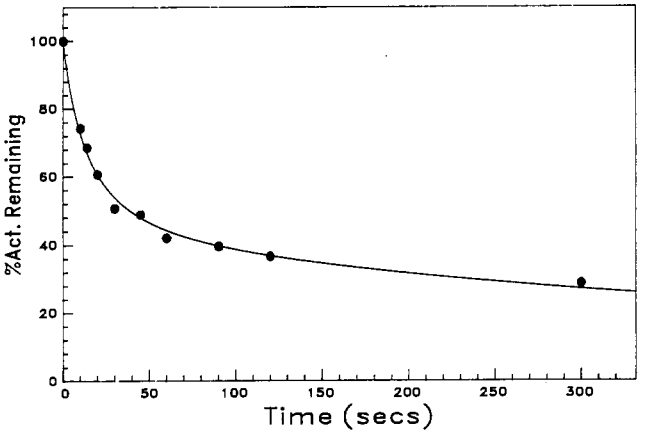

FIGURE 1: KINSIM simulation of the time-dependent inactivation of GS(n = 2) with PPT in the presence of Mn^{2+} at pH 6.5. The concentration of unadenylylated subunits and PPT was 8.3 μM. The experimental data are preresented by the solid dots, and the solid line is the simulation using the two-step mechanism shown in Scheme III with the association rates k_2 = 0.014 ± 0.001 μM^{-1} s^{-1} and k_5 = 0.0004 ± 0.0001 μM^{-1} s^{-1}. The simulations were insensitive to values assumed for the phosphoryl-transfer step.

Simulation of time-dependent inactivation data for GS(n = 2) with Mg^{2+} at pH 7.5 gave association rates for the two phases of the reaction of 0.012 μM^{-1} s^{-1} and 0.002 μM^{-1} s^{-1}, while those for GS(n = 12) with Mn^{2+} at pH 6.5 were found to be 0.007 μM^{-1} s^{-1} and 0.0006 μM^{-1} s^{-1}. These simulation results were for only one concentration of PPT.

Rapid Quench Experiments. Rapid quench experiments were conducted with use of either an equimolar concentration of PPT and enzyme or a very high concentration of PPT. KINSIM simulations of the high PPT concentration data shown in Figure 2A were insensitive to variations in the association rate of PPT but were very sensitive to the rate of phosphoryl transfer. At very high PPT concentrations, the rate of acid-labile phosphate formation is due solely to the rate of phosphoryl transfer, as the inhibitor association rate is now fast. KINSIM simulations of the low PPT concentration data shown in Figure 2B were sensitive to both the association rate of the inhibitor and the rate of phosphoryl transfer. At low PPT

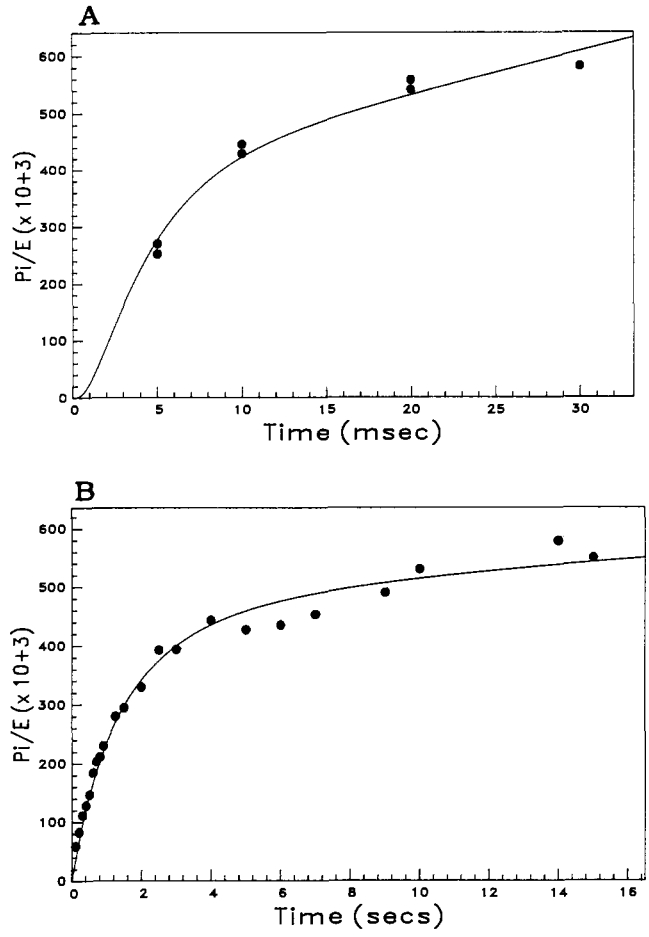

FIGURE 2: Rapid quench data for GS(n = 2) with PPT in the presence of Mn^{2+} at pH 6.5 and 25 °C. (A) Rapid quench data from a reaction containing 100 mM PPT, 62.5 μM unadenylylated GS subunits, 600 μM ATP, 100 mM KCl, 8 mM $MnCl_2$, and 200 mM Pipes at pH 6.5. Data was collected from 5 ms to 2 s. Data shown are those from 5 to 30 ms. Solid dots represent experimental data. The solid line is that from the KINSIM simulation using the mechanism in Scheme III and the rate constants in Table II. (B) Rapid quench data from a reaction containing 60 μM PPT and 59 μM unadenylylated GS subunits in the same buffer as above. Data were collected from 100 ms to 15 s.

concentrations therefore, the rate of formation of acid-labile phosphate is due to both the binding rate of the inhibitor and the phosphroyl-transfer rate.

Both sets of rapid quench kinetic data were simulated simultaneously by use of the mechanism shown in Scheme III. Values for the forward rate constants k_2, k_3, k_5, and k_6 were calculated, and the results of these calculations are summarized in Table II. The simulations are superimposed on the experimental data in Figures 1 and 2. The values obtained for k_2 and k_5 from simultating the rapid quench data are in good agreement with the rate constants for inhibitor association, which were obtained from simulation of the time-dependent inactivation data. The populations of the fast and slow enzyme species were again varied between 55–45% for the initial phase and 45–55%, respectively, for the slower phase. The best fit was achieved with 45% of the enzyme being inactivated in the fast initial phase and 55% being inactivated in the slower phase. The high PPT concentration experiment proceeded to 80% inactivation (data not shown), and there is some indication in these data that the inactivation rate continues to slow in the late stages of inhibition. However, in the experiment with low PPT concentrations, inactivation proceeded to 60% before the inactivation rate became too slow to measure accurately. It is quite possible that during the later stages of the inactivation the inhibition continues to slow down and that the second phase is really the average of many different smaller rate constants that are difficult to distinguish accurately from one another. Simulation of the low PPT concentration data alone did not provide a unique solution for the rate constants in Scheme III. The experiments with high PPT concentrations were necessary therefore to provide an independent measurement of the phosphoryl-transfer rate that could be used to constrain the fits to the data. Simulations designed to solve for the reverse rate constants k_{-3} and k_{-6} did not yield accurate values for these rate constants, which were found to range from 0.0 to 6.0 s^{-1}. Likewise, accurate values could not be obtained for k_{-2} and k_{-5} with these data (see above). The large rate constants for phosphoryl transfer compared to other steps in the reaction along with the irreversible nature of the reaction itself probably contribute to the inability to obtain accurate values for reverse rate constants, especially k_{-2} and k_{-5}.

Table III: Rate Constants from Fitting Rapid Quench Data for High and Low [PPT]

enzyme	k_2 (μM^{-1} s^{-1})	k_3 (s^{-1})
GS(n = 2) Mn^{2+}, pH 6.5	0.014 ± 0.001	245 ± 14
GS(n = 12), Mn^{2+}, pH 6.5	0.012 ± 0.001	47 ± 4
GS(n = 2), Mg^{2+}, pH 7.5	0.004 ± 0.001	23 ± 3

Similar experiments were carried out on GS(n = 2) with Mg^{2+} at pH 7.5 and GS(n = 12) with Mn^{2+} at pH 6.5 and were analyzed in a similar manner. The best fits of the low and high PPT concentration data were obtained by assuming that 30% of the enzyme was involved in the initial fast phase of the inhibition. In both of these cases, the inhibition was too slow to measure accurately after 60% completion, and so no kinetic information was available concerning the last phases of inhibition. Due to the population differences for each enzyme form, and the uncertainty in the kinetic data for the later stages of inhibition, only the kinetic data from the initial phase of inactivation are summarized in Table III for comparative purposes.

KINSIM fitting of all of the experimental data, both rapid quench data sets and time-dependent inactivation data, could be done in an iterative manner. Initially the high PPT concentration rapid quench data could be fit for k_3 and k_6 and time-dependent inactivation data could be fit for k_2 and k_5. These values could then be used as starting points for fitting both sets of rapid quench data simultaneously for all of the forward rate constants first and then for all of the reverse rate constants. Eventually, all three data sets can be fit simultaneously in order to refine the fits further. The best fits were obtained when all of the forward rate constants were varied as an unlinked group. The populations were initially estimated with use of values from the double-exponential analysis. Once one set of rate constants was obtained for a given population set, the populations could be varied and the entire iterative process repeated until the best fit was obtained.

Discussion

The present investigation was begun to characterize the kinetic nature of the inhibition of *E. coli* glutamine synthetase by phosphinothricin. The results in Table III clearly show that under the conditions of a time-dependent inactivation experiment, the rate-limiting step in the inhibition kinetics is not the chemical reaction but is the binding of the inhibitor and/or some slow conformational change associated with binding. This result is the same for all three forms of the enzyme examined although the kinetic details of the inhibition differ slightly for each. The binding ($k_1 \sim 2$ μM^{-1} s^{-1}) of ATP (Abell & Villafranca, 1991) to all three forms of GS is about

2 orders of magnitude faster than the binding of PPT, which means that nucleotide binding is not rate limiting. For the inhibitor PPT, GS(n = 2) with Mn^{2+} shows an association rate similar to that of GS(n = 12) with Mn^{2+}; however, the GS(n = 2) enzyme form has a much faster phosphorylation rate. GS(n = 12) with Mn^{2+} and GS(n = 2) with Mg^{2+} show similar phosphorylation rates while the magnesium form of the enzyme shows the slowest binding rate. The association rate, k_2, of the inhibitor appears to correlate with the type of metal ion used for activation. The metal ions play an intimate role in the conformational integrity of GS, with the most tightly bound of the two metal ions required for GS activity serving to maintain the catalytically active conformation of the enzyme. Mg^{2+} is thought to bind approximately 200-fold less tightly than Mn^{2+} (Denton & Ginsburg, 1970). If there is a slow conformational change upon binding of PPT, then it is probably not surprising that the more tightly bound Mn^{2+} ion might facilitate that conformational change faster than the less tightly bound Mg^{2+} ion.

The phosphorylation rates (Table III) among the different enzyme forms are a little more difficult to interpret. Rapid quench kinetic experiments have previously been carried out on all three forms of the enzyme using the normal substrates, ATP, glutamate, and ammonia (Abell & Villafranca, 1991); however, it is not valid to compare the biosynthetic reaction involving phosphorylation of glutamate with phosphorylation of PPT. At no time in the "normal" chemical mechanism for glutamine synthetase does the enzyme bind a tetrahedral moiety that is not phosphorylated. Providing the enzyme with PPT, a "mimic" of the tetrahedral intermediate, is equivalent to starting the reaction in midstream; the enzyme appears to use the added binding energy of the intermediate analogue, PPT, to facilitate phosphorylation of the inhibitor converting PPT to a true "mimic" of the normal phosphorylated tetrahedral intermediate. The rate constants for phosphoryl transfer to PPT are expected, therefore, to differ from those found for the normal enzymatic reaction where a phosphoryl group is transferred to a ground-state or slightly activated substrate (Knowles, 1980). In the present experiments, the data indicate that phosphroyl transfer to PPT is very heavily favored in the forward direction, consistent with the fact that the normal tetrahedral intermediate is a phosphorylated species throughout the entire course of the reaction. The fact that the inhibitor is not a perfect analogue of the tetrahedral intermediate (precisely because it is not initially phosphorylated) may account for its slow binding. It remains to be seen if PPT-P binds more rapidly than PPT to glutamine synthetase.

In a more qualitative sense, the results from the rapid quench experiments with the biosynthetic reaction may be used to understand the trend in phosphoryl-transfer rates of PPT (Abell & Villafranca, 1991). GS(n = 2) with Mn^{2+} appears from the results of the inhibition experiments to stabilize the transition state for phosphoryl transfer to PPT better than the other two forms of the enzyme. Superior stabilization of the transition state for phosphoryl transfer to glutamate was also observed for this form of the enzyme in the biosynthetic reaction compared to the other two forms of the enzyme. Both GS(n = 2) with Mg^{2+} and GS(n = 12) with Mn^{2+} appear to stabilize the transition state for phosphoryl transfer to PPT to a similar extent, and the same trend was observed with the biosynthetic reaction. The difference worth noting here is that in the case of the biosynthetic reaction GS(n = 12) did not stabilize the γ-glutamyl phosphate intermediate relative to the ternary complex, which resulted in a significant amount of reverse phosphoryl transfer; for this enzyme form phosphoryl transfer was the rate-limiting step. In the case of PPT, the enzyme is binding an "intermediate" that occurs along the reaction pathway after formation of the γ-glutamyl phosphate intermediate; therefore, whatever factors destabilized the γ-glutamyl phosphate intermediate do not appear to affect phosphoryl transfer to phosphinothricin.

The results of the complete kinetic analysis on GS(n = 2) with Mn^{2+} indicated that as the inhibition proceeded not only the binding rate of PPT but also the phosphorylation rate decreased. The physical implications of these results can be understood by inspection of the structure of glutamine synthetase. With each active site situated at the interface between two adjacent subunits (Yamashita et al., 1989), it is conceivable that any conformational changes at one active site would be readily communicated to other nearby active sites. In the case of the analogous inhibitor MSOX, partial inactivation of the enzyme results in a reduction in the rate of the conformational change observed upon removal of Mn^{2+} ions from the remaining subunits. This reduction in rate reflects the decreased flexibility of the unoccupied active sites, which are near those containing bound MSOX-P and ADP (Maurizi & Ginsburg, 1985). There is evidence from fluorescence studies of GS inactivation with PPT that a conformational change does occur during inactivation (Logusch et al., 1990). Conformational locking of a particular site by irreversible inhibition with PPT could well produce a "domino effect" resulting in altered binding of PPT to adjacent or nearby subunits. The data from the experiments with PPT were fit to a two-population model. In such a model, the first population that undergoes rapid initial inactivation represents completely uninhibited enzyme whereas the second population represents the dodecamer at some later stage of inhibition where some percentage of the active sites is already inhibited. There could of course be as many as 12 different populations of enzyme, each undergoing inactivation at a different rate. While the time-dependent inactivation data are not sensitive enough to detect more than two populations and represent average rates of inactivation over a given number of active sites, the rapid quench data suggest more than two populations.

It is clear from the results of these experiments that rate constants derived from time-dependent inactivation data for GS with PPT as well as similar transition-state analogues reflect the slow step of the inactivation process, the association rate of the inhibitor with the enzyme. Previous investigations from this laboratory have examined a number of α- and γ-substituted phosphinothricins, and rate constants were derived for each of these compounds from time-dependent inactivation experiments and fluorescence studies (Logusch et al., 1990). The rate constants for these compounds therefore reflect the association rate for enzyme only and not phosphorylation rates. The derived rate constants do not vary greatly with substitution pattern, indicating that substitutions at the α and γ positions do not significantly affect the association rate of the inhibitor. The electronic effects that these substitutions have on the rate of phosphoryl transfer have yet to be determined. Similar findings have been reported for other slow-binding inhibitors of other enzymes (Bunning, 1987; Merkler et al., 1990).

Phosphorylation of a tetrahedral inhibitor that mimics a phosphorylated tetrahedral intermediate is not unique to glutamine synthetase. D-Ala-D-Ala ligase is thought to proceed through the initial formation of the acyl phosphate of alanine followed by the formation of a tetrahedral intermediate between a second molecule of alanine and the activated acyl phosphate that collapses to form D-Ala-D-Ala and inorganic phosphate (Duncan & Walsh, 1988). Several (aminoalkyl)-

phosphinate analogues have been found to be potent inhibitors of this enzyme, but rapid quench kinetic data have not been reported for these inhibitors. These inhibitors show time-dependent inactivation and require ATP for inhibition. Recent rotational resonance studies have been used to detect the presence of the (aminoalkyl)phosphinate phosphate at the active site of D-Ala-D-Ala ligase (McDermott et al., 1990). The (aminoalkyl)phosphinate inhibitors, like PPT, mimic a tetrahedral intermediate that remains phosphorylated during the normal course of the reaction. It would not be surprising, therefore, if the kinetics for inactivation for the two cases were similar with relatively rapid phosphorylation of the inhibitor and with inhibitor binding and/or an associated conformational change being the rate-limiting step.

Rapid quench kinetic techniques have allowed the dissection of the complex inhibition kinetics exhibited by GS with PPT. Use of these techniques combined with KINSIM analyses has determined that the rate-limiting step in the inactivation is inhibitor association and that the inhibitor association rate correlates with the metal ion used for activation. In contrast, the adenylylation state of the enzyme appears to have more of an effect on the phosphoryl-transfer rate to PPT than the metal ion type. These experiments have provided the first elucidation of the rate of chemical modification of a transition state analogue.

ACKNOWLEDGMENTS

We thank John V. Schloss for suggesting the double-exponential analysis.

REFERENCES

Abell, L. M., & Villafranca, J. J. (1991) *Biochemistry 30*, 1413–1418.

Almassy, R. J., Janson, C. A., Hamlin, R., Xuong, N.-H., & Eisenberg, D. (1986) *Nature 323*, 304–309.

Backman, K., Chen, Y.-M., & Magasanik, B. (1981) *Proc. Natl. Acad. Sci. U.S.A. 78*, 3743–3747.

Barshop, B. A., Wrenn, R. F., & Frieden, C. (1983) *Anal. Biochem. 130*, 134.

Bunning, P. (1987) *J. Cardiovasc. Pharmacol. 10 (Suppl. 7)*, 531–535.

Colanduoni, J. A., & Villafranca, J. J. (1986) *Bioorg. Chem. 14*, 163–169.

Denton, M. D., & Ginsburg, A. (1970) *Biochemistry 9*, 617.

Duggleby, R. G. (1984) *Comput. Biol. Med. 14*, 447–455.

Duncan, K., & Walsh, C. T. (1988) *Biochemistry 27*, 3709–3714.

Ginsburg, A., & Stadtman, E. R. (1973) in *The Enzymes of Glutamine Metabolism* (Prusiner, S., & Stadtman, E. R., Eds.) pp 9–44, Academic Press, Inc., New York.

Ginsburg, A., Yeh, J., Hennig, S. B., & Denton, M. D. (1970) *Biochemistry 9*, 633.

Hennig, S. B., & Ginsburg, A. (1971) *Arch. Biochem. Biophys. 144*, 611.

Johnson, K. A. (1986) *Methods Enzymol. 134*, 677.

Knowles, J. R. (1980) *Annu. Rev. Biochem. 49*, 877–919.

Lewis, D. A., & Villafranca, J. J. (1989) *Biochemistry 28*, 8454.

Logusch, E. W., Walker, D. M., McDonald, J. F., & Franz, J. E. (1989) *Biochemistry 28*, 3043–3051.

Logusch, E. W., Walker, D. M., McDonald, J. F., Franz, J. E., Villafranca, J. J., DiIanni, C. L., Colanduoni, J. A., Li, B., & Schineller (1990) *Biochemistry 29*, 366–372.

Magasanik, B., & Reitzer, L. J. (1987) in *Escherichia coli & Salmonella Typhimurium—Cellular and Molecular Biology* (Neidhardt, F. C., Ed.) Vol. 1, pp 302–320, American Society for Molecular Biology, Washington, DC.

Maurizi, M. R., & Ginsburg, A. (1982) *J. Biol. Chem. 257*, 4271–4278.

Maurizi, M. R., & Ginsburg, A. (1985) in *Curr. Top. Cell Regul. 26*, 191–206.

McDermott, A. E., Creuzet, F., Griffin, R. G., Zawadzke, L. E., Ye, Q.-H., & Walsh, C. T. (1990) *Biochemistry 29*, 5767–5775.

Merkler, D. J., Brenowitz, M., & Schramm, V. L. (1990) *Biochemistry 29*, 8358–8364.

Meek, T. D., & Villafranca, J. J. (1980) *Biochemistry 19*, 5513–5519.

Meek, T. D., Johnson, K. A., & Villafranca, J. J. (1982) *Biochemistry 21*, 2158–2166.

Miller, R. E., Shelton, E., & Stadtman, E. R. (1974) *Arch. Biochem. Biophys. 163*, 155–171.

Morrison, J. F., & Walsh, C. T. (1988) *Adv. Enzymol. Relat. Areas Mol. Biol. 61*, 201–301.

Rhee, S. G., Chock, P. B., & Stadtman, E. R. (1985) *Methods Enzymol. 113*, 213.

Ronzio, R. A., & Meister, A. (1968) *Proc. Natl. Acad. Sci. U.S.A. 59*, 164.

Ronzio, R. A., Rowe, W. B., & Meister, A. (1969) *Biochemistry 8*, 1066.

Roseman & Levine (1987) *J. Biol. Chem. 262*, 2101.

Rowe, W. B., Ronzio, R. A., & Meister, A. (1969) *Biochemistry 8*, 2674.

Schineller, J. B., & Villafranca, J. J. (1991) *J. Am. Chem. Soc.* (submitted for publication).

Shrake, A., Ginsburg, A., Wedler, F. C., & Sugiyama, Y. (1982) *J. Biol. Chem. 257*, 8238–8243.

Stadtman, E. R., & Ginsburg, A. (1974) in *The Enzymes* (Boyer, P. D., Ed.) Vol. 3, p 755–807, Academic Press, Inc., New York.

Stadtman, E. R., Smyfniotis, P. Z., Davis, J. N., & Wittenberger, M. E. (1979) *Anal. Biochem. 85*, 275.

Stadtman, E. R., Mura, E., Chock, P. B., & Rhee, S. G. (1980) in *Glutamine: Metabolism, Enzymology, & Regulation* (Mora, J., & Palacios, R., Eds.) pp 41–59, Academic Press, Inc., New York.

Yamashita, M. M., Almassy, R. J., Janson, C. A., Cascio, D., & Eisenberg, D. (1989) *J. Biol. Chem. 264*, 17681–17690.